Environmental Toxicology and Pharmacology 108 (2024) 104459

Contents lists available at ScienceDirect

Environmental Toxicology and Pharmacology

journal homepage: www.elsevier.com/locate/etap

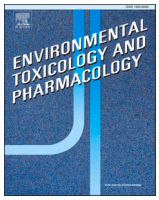

Occupational second-hand smoke exposure: A comparative shotgun proteomics study on nasal epithelia from healthy restaurant workers

Sofia Neves [a,b,*,1], Solange Pacheco [a,1], Fátima Vaz [a,b], Peter James [c], Tânia Simões [d], Deborah Penque [a,b]

[a] Laboratory of Proteomics, Human Genetics Department, National Institute of Health Dr. Ricardo Jorge, INSA I.P, Lisbon, Portugal
[b] Center for Toxicogenomics and Human Health, ToxOmics, NOVA Medical School-FCM, UNL, Lisbon, Portugal
[c] Protein Technology Laboratory, Department of Immunotechnology, Lund University, Sweden
[d] CECAD Cologne-Excellence in Aging Research University of Cologne, Germany

ARTICLE INFO

Keywords:
Cigarette smoke
Second-Hand Smoke
Protein network
Mass Spectrometry
Nasal epithelium
Proteomics

ABSTRACT

Non-smokers exposed to second-hand smoke (SHS) present risk of developing tobacco smoke-associated pathologies. To investigate the airway molecular response to SHS exposure that could be used in health risk assessment, comparative shotgun proteomics was performed on nasal epithelium from a group of healthy restaurant workers, non-smokers (never and former) exposed and not exposed to SHS in the workplace. HIF1α-glycolytic targets (GAPDH, TPI) and proteins related to xenobiotic metabolism, cell proliferation and differentiation leading to cancer (ADH1C, TUBB4B, EEF2) showed significant modulation in non-smokers exposed. In never smokers exposed, enrichment of glutathione metabolism pathway and EEF2-regulating protein synthesis in genotoxic response were increased, while in former smokers exposed, proteins (LYZ, ATP1A1, SERPINB3) associated with tissue damage/regeneration, apoptosis inhibition and inflammation that may lead to asthma, COPD or cancer, were upregulated. The identified proteins are potential response and susceptibility/risk biomarkers for SHS exposure.

1. Introduction

Second-hand Smoke (SHS), also known as passive smoking, involuntary smoking or environmental tobacco smoke, is a hazard environment pollutant, especially when concentrated in indoors spaces. SHS is originated from the act of burning tobacco, mostly from a cigarette. Long-term exposure to SHS can lead to severe and fatal diseases like coronary heart disease, stroke, lung cancer, breast cancer, Chronic Obstructive Pulmonary Disease (COPD) and diabetes (Carreras et al., 2019). According to the World Health Organization (WHO), there is no risk-free level of exposure to SHS. WHO estimates that each year about 1.2 million deaths result from SHS exposure by non-smokers (World Health Organization, 2019).

Current Portuguese legislation bans tobacco smoking in all public indoor places (Law 109/2015). However, before 2015, the Portuguese Smoking law was partial (Law 37/2007), allowing indoor smoking areas in bars and restaurants. The designated smoking areas of some of these restaurants were significantly contaminated with high levels of particular matter $PM_{2.5}$ compatible with tobacco smoke, despite imposed protection requirements, as we previously demonstrated (Pacheco et al., 2012). Non-smoker employees working in these areas showed elevated levels of cotinine, a nicotine metabolite, in their urine, confirming their exposure to SHS (Marques et al., 2021; Pacheco et al., 2012). By challenge-comet assay, we showed that the lymphocytes from those restaurant workers exposed to SHS presented a modified response to a genotoxic challenge, consistent with an adaptive response (Vital et al., 2021). Plasma acute phase inflammation proteins, such as ceruloplasmin (CP) and inhibitor of inter-alpha-trypsin heavy chain 4 (ITIH4) that may precede the onset of SHS related diseases, were also changed in those non-smoker workers exposed to SHS (Pacheco et al., 2013).

The objective of the present work is to investigate the molecular effects of SHS occupational exposure on the respiratory tract proteome of those non-smokers employees (e.g., never and former smokers) exposed *versus* non-exposed ones. A group of smokers working in restaurants where smoking was not allowed was used as basis of

* Corresponding author at: Laboratory of Proteomics, Human Genetics Department, National Institute of Health Dr. Ricardo Jorge, INSA I.P, Lisbon, Portugal.
E-mail address: sofia.neves@insa.min-saude.pt (S. Neves).
[1] both authors contributed equally to this study

https://doi.org/10.1016/j.etap.2024.104459
Received 26 December 2023; Received in revised form 5 April 2024; Accepted 22 April 2024
Available online 27 April 2024

comparison for identification of SHS exposure associated proteins.

Given the inherent difficulties to have access to bronchial epithelia, we focused our study on the nasal epithelia, which has been demonstrated to be a suitable and easily collected cell model to study airway diseases as those induced by tobacco smoke (Gower et al., 2011; Simões et al., 2011; Sridhar et al., 2008).

By using a shotgun proteomics approach on the nasal epithelia, we uncovered protein signatures associated with SHS exposure effects that seemed to be different in former smokers compared to never smokers exposed to SHS. These protein signatures can be a start point for biomarker development to assess and prevent the risk for the onset of respiratory diseases related to tobacco smoke exposure.

2. Materials and Methods

2.1. Experimental design

This is a cross-sectional study carried out using a shotgun proteomics approach on a biobank of nasal epithelium samples obtained from employees of a group of Lisbon restaurants or canteens, with/without smoking free rooms (under Smoking Legislation prior to 2015). The air quality of these venues, and the demography and clinical evaluation of the workers, including spirometry and urinary cotinine measurements, were previously reported (Pacheco et al., 2013, 2012). Nasal epithelium samples were obtained by brushing technique and pre-evaluated by cytology, as previously described (Penque et al., 2000), and stored in PBS at -80^0 C until further analysis. For proteomics analysis, samples from 48 workers meeting the following criteria were selected: i) normal values of spirometry, ii) no declared respiratory disease, iii) more than 20 hours per week of working time together with at least a year of permanence at current workplace, iv) cigarette SHS exposure of at least 1-year and v) former smoking habit with at least 6 months of abstinence. Samples were classified as smokers (**S**) not exposed to SHS at the workplace (n=8), and non-smokers (n=40), in which 19 were not exposed (**NS**) and 21 were exposed to SHS (**NSE**). **NS** was subgrouped into 11 "Never Smokers" (**N**) and 8 "Former Smokers" (**F**), and the **NSE** into eleven 11 "Never Smokers Exposed" (**NE**) and 10 "Former Smokers Exposed" (**FE**) to SHS (see Fig. 1 for the schematic diagram).

This study was approved by the Ethics Committee of the National Institute of Health Dr. Ricardo Jorge, INSA I.P, Lisbon, Portugal. Written informed consent was obtained from all volunteers.

2.2. Sample Preparation

Samples were thawed and lysed at 4 °C in 130 µL of lysis buffer (10 mM Tris-HCl pH 7.4, 2 mM EDTA, SDS1% and 20 mM NaCl), with intermittent sequences of 1' of vortex followed by 2' of heating at 95 °C and ultrasound sheared force at Room Temperature (RT). Samples were left in lysis buffer overnight at 4 °C, and then spun down at 16,100 xg (1' at 4 °C). The supernatant was collected, centrifuged at 16,100 xg (1' at 4 °C) and protein quantified by Bicinchoninic Acid (BCA) protein assay. 10 µg of total protein of each sample was briefly separated by 12% SDS-PAGE (Mini-PROTEAN® TGX™, Bio-Rad Laboratories), until migration into one single band. Gel was stained using GelCode blue (Thermo Fisher Scientific Inc.) and the stained band/sample was cut into nine cubes (1 mm^3). The slices were distained with 50% Acetonitrile (ACN) and 25 mM Ammonium Bicarbonate (AmBic), 2×30′ at RT; and proteins were then reduced by 10 mM Dithiotreitol (DTT) in 100 mM AmBic for 1 h at 57 °C, and alkylated with 55 mM Iodoacetamide (IAA) in 100 mM AmBic for 45′at RT, in the dark. Slices were washed twice with 100 µL of 100 mM AmBic followed by ACN 100% dehydration by freeze speed-vac (T<0°C) (SpeedVac ™ SRF110, Thermo Fisher Scientific) and digestion with 150 µL of Sequencing grade modified trypsin (Promega Biotech AB) (12.5 ng/µL in 50 mM AmBic) for 12 h at 37 °C. Peptides were extract from the gel slices by incubation in 200 µL of 75% ACN and 5% Trifluoroacetic acid (TFA) 2×30' at RT, under vortex, followed by the incubation with 200 µL of ACN 100% for 10' and then freeze dehydration by speed-vacuum (T<0°C). Samples were stored at - 80 °C until MS analysis.

2.3. LC-MS/MS protein separation

Before analysis, samples were re-suspended in 0.1% Formic Acid (FA) for 30' and subjected to C18 spin column-based cleaning procedure (The Nest Group, Inc., USA). An ESI-LTQ-Orbitrap XL mass spectrometer (Thermo Fisher Scientific Inc.) interfaced with an Eksigent nanoLC 2DTM and HPLC system (Eksigent technologies) was used for all samples. A total of 5 µL (2.5 µg of protein digests) were loaded, trapped and washed with a constant flow rate of 10 µL/minute with 0.1% FA, for 15' onto a pre-column (PepMap 100, C18, 5 µM, 5 mm×0.3 mm; LC Packings, Amsterdam, Netherlands). The peptides were subsequently separated on a 10 µM fused silica emitter, 75 µM x 16 cm (PicoTip™ Emitter), packed in-house with Reprosil-Pur C18-AQ resin (3 µM; Dr Maisch, Ammerbuch-Entringen). Peptides were eluted with a flow rate of 300 nL/minute with a 60' linear gradient of 3–35% (v/v) ACN in water, containing 0.1% (v/v) FA and then increased rapidly to 90%

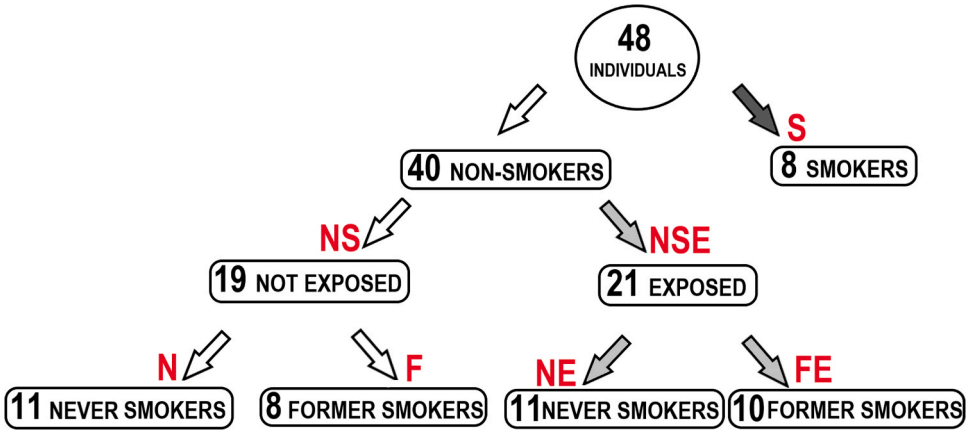

Fig. 1. Classification/subdivision of the cohort according to the worker's smoking habits and exposure to SHS in the workplace. In total, 48 healthy employees working in different Lisbon restaurants/canteens were selected for the study. From these, 40 were non-smokers and 8 smokers (S). In non-smoker group, 19 were classified as not exposed to SHS (NS) and 21 as non-smoker exposed (NE). NS group was subgrouped into 11 never smokers not exposed (N) e 8 former smokers not exposed (F). NSE was subgrouped into 11 never smokers exposed (NE) and 10 former smokers exposed (FE). Dark grey arrows demark smoker group; white arrows indicate non-smokers and non-smokers not exposed, and light grey arrows indicate the non-smoker groups exposed to SHS.

(until 68′) and was kept until 78′, before re-equilibrating. A blank LC-MS/MS run was performed between each analysed sample. The LTQ-Orbitrap was operated in data-dependent mode (DDA) to automatically switch between Orbitrap-MS (up to 2000 Da) and LTQ-MS/MS (between 50 and 2000 Da) acquisition. Mass spectra of all samples was acquired in the positive ionization mode. Four MS/MS spectra were acquired in the linear ion trap per each FT-MS scan, which was obtained at 60,000 FWHM nominal resolution settings using the lock mass option (m/z 445.120025) for internal calibration. The DDA was performed with dynamic exclusion. The dynamic exclusion list was restricted to $N_{\text{entries}} = 500$; using $N_{\text{repeat count}} = 2$; with an $N_{\text{repeat duration}} = 20''$ and an $N_{\text{dynamic exclusion range}} = 2'$ after the 2nd peptide count. Precursor ion "charge state screening" was enabled, to select for ions with at least two charges and rejecting ions with undetermined charge state. The CID energy was set to 35%, and one micro scan acquired for each spectrum. Data was acquired using the Xcalibur (version 2.0.7).

2.4. Selected Reaction Monitoring (SRM) assay

To quantify a target protein, an SRM assay was developed in Skyline (version 2.6) (MacLean et al., 2010). The peptides were checked against a theoretical peptide database that included those with 7–25 amino acid length obtained from a human proteome, fetched from UniProt KB database (Consortium, 2023). Synthetic peptides were spiked to validate the peak selection. The peptides were solubilized according to manufacturer's instructions and a pool of peptides was produced with a final concentration of 250 fmol/μL. 2 μL of that mixture were spiked in 8 μL of peptide samples from the nasal epithelium. An Eksigent 2D NanoLC system connected to a Triple Stage Quadrupole Mass Spectrometer (TSQ Vantage), with a Nano-ElectroSpray Interface was used for LC-SRM analysis. Solvents used were mobile phase A (mobA) and phase B (mobB), which is, H_2O/0.1% FA (v/v) and ACN/0.1% FA (v/v), respectively. The LC system was equipped with a trap column (0.3 mm id, 5 mm, PepMap Acclaim C18; LC Packings) and in-house packed analytical columns, in 0.075 mm id, 100 mm PicoFrits (New Objective), with 3 μM ReproSil C18-AQ particles (Dr Maisch, Ammerbuch-Entringen), to a length of 12 cm. A 300 nL/minute linear LC gradient delivered mobA, starting with 97%, then decreasing to 85% during 6', and then further down to 65% during 68'. An injection, for wash and equilibration of the column was perform between each sample. The TSQ operated in the positive ion mode with a spray voltage of 1.8 KV and an ion capillary temperature of 270 °C. A 0.7 Da unit resolution, for both Q1 and Q3 were set, as well as 10 ms dwell time per transition. Data acquired from Xcalibur were imported to Skyline to be analysed and manually inspected. Peak areas, for the measured SRM transitions for each individual peptide, were integrated and summed to generate the peptide peak areas. After data normalization using the software Normalyzer (http://quantitativeproteomics.org/normalyzer.) (Chawade et al., 2014), the data was imported to IBM SPSS (version 22) for statistical testing, where the normally distributed data was analysed by two-sided Student's t test.

2.5. Mass spectra data analysis

2.5.1. PatternLab software in protein identification and quantification

Peptide spectrum matching (PSM) was achieved by the Search Engine Comet (version 2016.01 rev. 3) in PatternLab for Proteomics (http://patternlabforproteomics.org) (version 4.1.1.4) (Carvalho et al., 2016). From the UniProtKB (https://www.uniprot.org), and restricted to the reviewed Swiss-Prot (ID UP000005640), a *Homo sapiens* (ID 9606) proteins database was retrieved in 28/06/2018 (Consortium, 2023). To this database 127 common contaminants were added. To control FDR a "reverse" decoy database was used. The parameters for the Comet Search Engine were: B, Y and NL precursors MS1 ions, trypsin "fully specific" digestion with only two (2) missed cleavage tolerance, a 600–5500 Da search mass range, with a precursor mass accuracy of 40 ppm and a MS/MS bin tolerance of 1.0005 m/z, using only cysteine carbamidomethylation as a fixed post-translational modification (PTM), with no variable PTMs.

To obtain reliable protein identification Comet's results were submitted to the default processing quality filters of Search Engine Processor (SEPro) for "High Resolution MS1" with minor modifications: in "Pre-Processing Quality Filter" the "DeltaMass PPM" with value 30.0 and "DeltaCN" with 0.0010 but with a 5 minimum number of amino acids residues of possible solutions. SEPro resorts to the application of a Bayesian discriminator, a three-tier Bayesian algorithm. Default options of 3, 2, and 1% for the false discovery rate (FDR) were chosen for spectral, peptide and protein level filtering, respectively. After filtering, all identified proteins with at least one peptide (1 PSM), a minimum 1.8 Bayesian Score and a maximal difference of 10 in "DeltaMass PPM" from Avg PPM", were selected. The final list of inferred proteins had to fit two criteria: i) proteins had to present at least one unique peptide and two degenerative peptides and ii) identified proteins had to be detected in at least 80% of each group or subgroup of individuals.

For label-free relative quantification, PatternLab's XIC extraction was used, where the area under the curve of the extracted-ion chromatograms (XIC) of the identified peptides was taken as a comparative tool for measurement. The quantities were normalized by a "normalized ion abundance factor" approach - NIAF (Carvalho et al., 2016, 2013).

2.5.2. Network mapping

Proteins identified in ≥ 80% of subjects in a group or subgroup were selected for a single or multiple cluster comparison analysis, using the ClueGO's functional analysis algorithm (http://www.ici.upmc.fr/cluego/cluegoDownload.shtml) (version 2.5.9) in Cytoscape software (https://cytoscape.org/index.html). "Biological terms" (GO term "Biological process") and pathways specifically enriched for each group or subgroups were determined by cluster analysis, as described in Mlecnik et al., (2018) and Trindade et al., (2019). A pathway/biological process was established as specifically enriched in a (sub)group when more than 60% of proteins are from that (sub)group-specific cluster (list of proteins). From this analysis, a network of proteins and respective functions was retrieved using several public databases: "Kyoto Encyclopedia of Genes and Genomes" (KEGG) (https://www.genome.jp/kegg/), Gene Ontology Knowledgebase (GO) (http://geneontology.org/) REACTOME (https://reactome.org/), and Wikipathways (https://www.wikipathways.org). In all of these databases, information obtained from all experimental data and inferred from "Reviewed Computational Analysis" was selected. Default ClueGO parameters were used, with the exception of "Network Specificity" (Min GO Level = 5 and Max GO Level = 11), "GO term fusion" ("parent-child" fusion) and "Kappa Score" (threshold of 0.9). Statistically significant pathways (p-value≤0.05) were determined by a two-sided hypergeometric test, using the Bonferroni step down correction for p-value adjustment.

2.6. Statistical analysis

Statistical analysis based on nonparametric tests was performed using IBM SPSS Statistics (version 27) and Microsoft Excel (version 2016) software. Significant modulation of clinical data parameters was discerned by Kruskal Wallis Test followed by Mann-Whitney U test. Bonferroni adjustment was conducted for multiple comparison correction. Differentially abundant proteins between groups were determined by Mann-Whitney U Test. The accepted alpha (α) level was 0.05. Continuous variables are represented by median with range or quartiles (25th, 50th, 75th) interval. The Venn diagram was acquired using a software available online (http://www.interactivenn.net/).

Table 1
Demographic Data.

PARAMETERS	DEMOGRAPHIC DATA								
	OCCUPATIONAL SECONDHAND SMOKE EXPOSURE								
	Never Smokers (N)	Never Smokers Exposed (NE)	Mann-Whitney U Test	Former Smokers (F)	Former Smokers Exposed (FE)	Mann-Whitney U Test	Smokers (S)	Kruskal-Wallis Test	
Subjects (n)	11	11	na	8	10	na	8	na	
Age (years)	42.0 [19;66]	33.0 [23;48]	retain null hypothesis	48.0 [26;63]	33.5 [25;57]	retain null hypothesis	44.0 [34;62]	retain null hypothesis	
Gender (F|M)	4|7	1|10	na	3|5	2|8	na	3|5	na	
Body mass index (kg/m^2)	25.8 [22.2;31.5]	24.5 [18.9;34.8]	retain null hypothesis	24.6 [21.2;28.7]	25.4 [20.3;31.3]	retain null hypothesis	24.7 [18.0;29.7]	retain null hypothesis	
Pulmonary function									
FVC (%)[a]	87.0 [75;98]	93.0 [80;105]	retain null hypothesis	100.0 [79;112]	96.5 [75;123]	retain null hypothesis	102.5 [78;149]	p<0.05	N *vs* F p<0.05 N *vs* S p<0.05
FEV_1 (%)[b]	91.0 [72;102]	96.0 [79; 104]	retain null hypothesis	98.5 [74;120]	94.5 [67,124]	retain null hypothesis	97.0 [74;140]	retain null hypothesis	
FEV_1 /FVC (%)[c]	81 [73;90]	83 [73;94]	retain null hypothesis	81.5 [71;88]	79.5 [69;93]	retain null hypothesis	76.5 [70;84]	retain null hypothesis	
Tobacco smoking									
Smoking habit duration (years)	na	na	na	11.0 [1;30]	6.0 [1;22]	retain null hypothesis	30.5 [18;48]	p<0.05	F *vs* FE p<0.001 S *vs* FE p<0.001
Cigarrete number per day	na	na	na	7.8 [1;20]	6.6 [1;80]	retain null hypothesis	12.5 [5;20]	retain null hypothesis	
Smoking withdrawal duration (years)	na	na	na	14.0 [2;23]	13.0 [1;36]	retain null hypothesis	na	na	
Urine Cotinine (ng/mL)	5.0 [5.0;6.0]	8.4 [5.0;27.9]	p<0.05	5.0 [5;10]	5.7 [5.0;7.1]	retain null hypothesis	1358.9 [513.0;2324,6]	p<0.001	N *vs* NE p<0.05 F *vs* NE p<0.05 N *vs* S p<0.001 F *vs* S p<0.001 NE *vs* S p<0.05 FE *vs* S p=0.001
Time in workplace (years)	2.0 [0.3;34]	5.0 [0.3;11]	retain null hypothesis	10.5 [3;21]	2.3 [1;34]	retain null hypothesis	9 [0.3;41]	retain null hypothesis	
Working time (hours/week)	40.0 [5;60]	40.0 [20;50]	retain null hypothesis	50.0 [40;60]	40.0 [14;40]	p<0.001	40.0 [40;66]	p<0.05	NE *vs* F p<0.05 FE *vs* F p<0.001
[PM2.5] at work place (µg/m^3)									
Maximum	38.0 [25;153]	220.0 [131;309]	p<0.001	48.0 [28;119]	247.0 [164;693]	p<0.001	100.50 [47;153]	p<0.001	N *vs* FE p<0.001 F *vs* NE p<0.001 S *vs* NE p<0.05 S *vs* FE p<0.05 N *vs* NE p<0.001 F *vs* FE p<0.001

na - not applicable
[a] Forced volume vital capacity (the determination of the vital capacity from a maximally forced expiratory effort)
[b] Volume that has been exhaled at the end of the first second of forced expiration
[c] Tiffeneau-pinelli index (expressed as FEV1%)

3. Results

3.1. Studied Cohort

Following our pre-established criteria, samples from 48 employees were selected for proteomics study. Samples were classified into three main groups, "Non-Smokers" (**NS**), "Non-Smokers Exposed" (**NSE**) and current "Smokers" (**S**), or into five subgroups, "Never Smokers" (**N**), "Never Smokers Exposed" (**NE**), "Former Smokers" (**F**), "Former Smokers Exposed" (**FE**) and current Smokers (**S**) (see Fig. 1). Demographic, clinical and epidemiological data of the five subgroups are shown in Table 1.

Selection of subjects did not specifically account for gender. A predominance of male individuals (73%) was observed. The median age varies between 33 and 48 years old among subgroups, without a statistically significant difference among them (Table 1.). Individuals had no respiratory diseases and no intake of respiratory related medication. Although significant differences were observed in spirometry values for "Forced Vital Capacity" (FVC) between the different subgroups, the FEV1/FVC ratio (forced expiratory volume in one second for FVC) was within the normal range in all subgroups, confirming that all individuals had normal pulmonary respiratory function.

The subgroups F and FE presented a median of 13 and 14 years of cigarette smoking abstinence, with a previous smoking habit that lasted 11 and 6 years, smoking 7.8 and 6.6 cigarettes per day, respectively. In contrast, the S group presented a higher cigarette smoking burden with a median of 12.5 cigarettes smoked per day and a median of 30.5 years of tobacco consumption.

The urinary cotinine levels were measured at the time of sample collection. N and F showed normal expected cotinine levels compatible with the non-smoking habit cut-off ($\leq$ 5 ng/mL). In contrast, NE presented significantly slightly higher levels of this molecule when compared with N, with a median of 8 ng/mL. FE although slightly higher, did not show a significant difference in the level of urinary cotinine when compared with the control subgroup F. As expected, S showed the highest concentrations, with a cotinine median of

1358.9 ng/mL (Table 1).

Most subgroups of workers had an average of 40 hours/week of work and between 2 and 10.5 years of work in the places of study. Air quality characterized by the presence of fine particle matters ($PM_{2.5}$), an indicator for air pollution associated to cigarette smoking, varied significantly between smoking and non-smoking workplaces. The subjects classified as N or F were workers of venues, where smoking was not permitted, while subjects classified as NE or FE subgroups worked in venues where smoking were allowed. $PM_{2.5}$ level was previously identified by us as significantly higher in smoking compared with those non-smoking venues (Table 1).

3.2. Nasal Epithelium Proteome Characterization - Functional annotation of proteins identified by shotgun proteomics

A total of 6552 tryptic peptides were detected, corresponding to a sum of 330 proteins identified under the pre-established criterion, one unique peptide plus two degenerative peptides.

Protein enrichment analysis was established using biological processes and pathways associated with the nasal epithelium proteome, through ClueGO application in Cytoscape (Fig.SI1(A) and Fig.SI1 (B&C)).

Fig. 2 displays the biological processes and pathways with more representability and probability of association connected with the queried proteins found in the nasal epithelium, including the top 5 most significant terms: "humoral immune response" (GO:0006959), "cellular oxidant detoxification" (GO:0098869), "cellular detoxification" (GO:1990748), "antimicrobial humoral response" (GO:0019730) and "Glycolysis/ Gluconeogenesis" (KEGG:00010).

Biological processes associated with the cross talking that may happen between the nasal epithelium and the Immune System were globally overrepresented. Cellular detoxification, a biological process connected with reactive oxygen species (ROS), such as hydrogen peroxide, were also highlighted. As expected, some proteins were related to "Drug metabolism" and "Metabolism of xenobiotics by cytochrome P450" pathways since the nasal epithelium is one of the 1st barriers in contact with airborne polluting agents.

3.3. Nasal Epithelium Proteome Exposed to SHS

To uncover reliable differential proteins associated with a specific biological condition, an additional identification criterion was established to minimize any eventual technical variability in protein identification: proteins should be detected in at least 80% of each group or subgroup. As a result, a more restrictive number of proteins were selected for further statistical analysis: 108 total for the groups and 124 total proteins for the subgroups.

Fig. 3 shows Venn diagrams of the protein's distribution among the three groups, NS, NSE and S (Fig. 3**A**), or the five subgroups, N, NE, F, FE and S (Fig. 3**B**).

The list of proteins identified in each group and subgroup is shown in supplementary Table SI1. Table 2 shows proteins that were found exclusively in more than 80% of subjects of NSE group, and NE and FE subgroups. These proteins were considered as specific for that (sub) group.

3.3.1. Functional annotation

The results of the network enrichment by cluster analysis and the associated proteins resulting from the comparison NSE *versus* NS groups (Fig.SI2(A), Fig.SI2(B) and Fig.SI2(C)) are summarized in Table 3. Similarly, the results from the comparisons NE *versus* N (Fig.SI3(A), Fig. SI3(B), Fig.SI3(C)) and FE *versus* F (Fig.SI4(A), Fig.SI4(B) and Fig.SI4 (C)) are represented in Table 4.

NSE group's proteome was specifically enriched (> 60% protein association in NSE cluster) with the following biological processes and pathways: "HIF1A and PPARG regulation of glycolysis" (WP:2456), "glutathione peroxidase activity" (GO:0004602), "Glutathione metabolism" (KEGG:00480), "granulocyte chemotaxis" (GO:0071621), "Propanoate metabolism" (KEGG:00640), "nicotinamide nucleotide metabolic process" (GO:0046496) and "Chemical carcinogenesis" (KEGG:05204). The Pathway "HIF1A and PPARG regulation of glycolysis" was associated with NSE-specific protein L-lactate dehydrogenase A chain protein (LDHA), while "glutathione peroxidase activity" process showed association with Glutathione S-transferase kappa 1 protein (GSTK1). "Glutathione metabolism" pathway was linked to GSTK1 and 6-phosphogluconate dehydrogenase, decarboxylating (PGD) (Table 3).

The NS group proteome was showed specifically enriched by "Thyroid hormone synthesis" (KEGG:04918) and "Carbohydrate digestion and absorption" (KEGG:04973) pathways. The former pathway was associated with Sodium/potassium-transporting ATPase subunit beta-1 (ATP1B1) and disulfide-isomerase A4 (PDIA4) proteins and the latter with ATP1B1 and Hexokinase-1 (HK1) NS-specific proteins (Table 3).

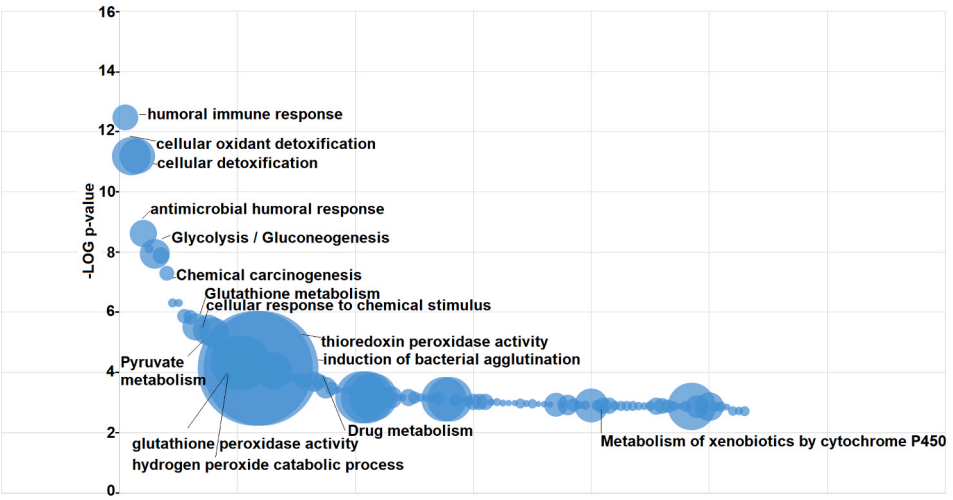

Fig. 2. Bubble chart representing the main biological processes identified in nasal epithelium proteome. Each circumference (bubble) represents a biological process. Larger bubbles indicate a higher percentage of identified proteins that belong to the biological process or pathway. The variable on the y-axis is given by the $-Log_{10}$ of the p-value and describes the probability of the biological process/pathway being linked to the analysed proteome. The probability is obtained from a two-sided hypergeometric test with Bonferroni step down correction (analysis in Cytoscape with application ClueGO using the ontologies: KEGG, Reactome and GO (Biological process); with 13237 total unique genes tested as described in (Mlecnik et al., 2018)).

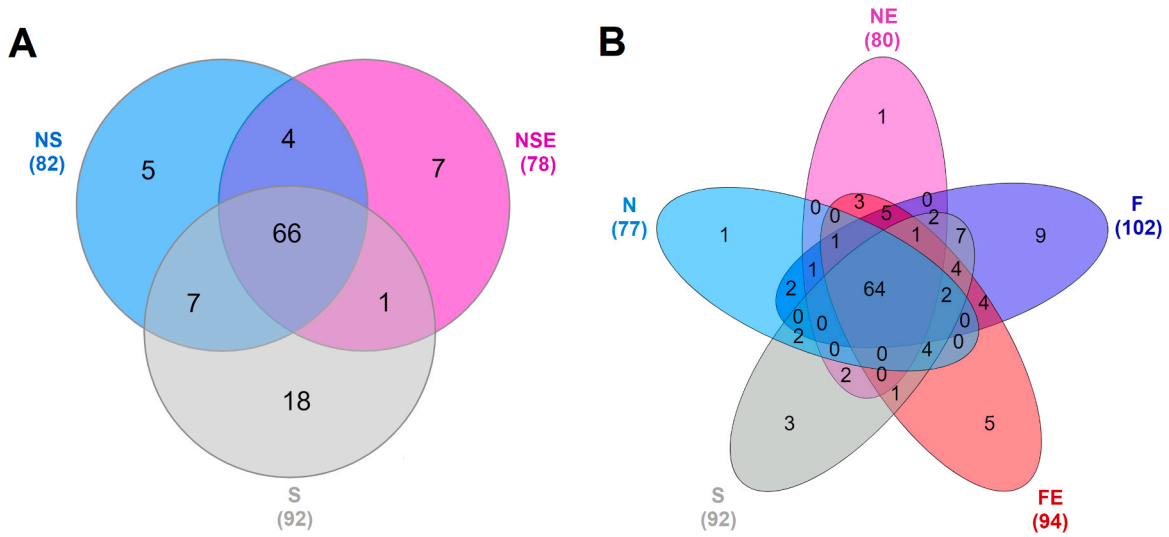

Fig. 3. Venn diagram of proteins detected in ≥ 80% in each group or subgroup. (**A**) Protein distribution among the three main groups: "Non-Smokers" (NS) not exposed and "Non-smokers Exposed" (NSE) to SHS and "Smokers" (S). (**B**) Protein distribution among the five subgroups: "Never Smokers" not exposed (N), "Never Smokers Exposed" (NE), "Former Smokers" not exposed (F) and "Former Smokers Exposed" to SHS (FE) and Smokers (S). Venn diagram was obtained by the online software http://www.interactivenn.net/.

Table 2
Proteins identified exclusively in the SHS exposed (sub)groups.

NSE Specific		
Uniprot Acession Number	**Gene Name**	**Protein Name**
P00338	LDHA	L-lactate dehydrogenase A chain
P17931	LGALS3	Galectin-3
P18124	RPL7	60 S ribosomal protein L7
P52209	PGD	6-phosphogluconate dehydrogenase decarboxylating
Q00839	HNRNPU	Heterogeneous nuclear ribonucleoprotein U
Q02878	RPL6	60 S ribosomal protein L6
Q9Y2Q3	GSTK1	Glutathione S-transferase kappa 1
NE Specific		
Uniprot Acession Number	**Gene Name**	**Protein Name**
P31946	YWHAB	14–3–3 protein beta/alpha
FE Specific		
Uniprot Acession Number	**Gene Name**	**Protein Name**
O75874	IDH1	Isocitrate dehydrogenase [NADP] cytoplasmic
P00403	MT-CO2	Cytochrome c oxidase subunit 2
P68431	HIST1H3A	Histone H3.1
Q00839	HNRNPU	Heterogeneous nuclear ribonucleoprotein U
Q96TA1	FAM129B	Niban-like protein 1

The proteome of NE subgroup showed association with "regulation of protein dephosphorylation" (GO: 0035304) and "Glutathione metabolism" (KEGG: 00480). This last pathway was found to be linked with the NE-specific proteins GSTK1 and PGD.

The N subgroup's proteome was specifically associated with "humoral immune response" (GO: 0006959), "Neutrophil extracellular trap formation" (KEGG: 04613), "antimicrobial humoral response" (GO: 0019730), "IL-17 signalling pathway" (KEGG: 04657), "Vitamin B12 metabolism" (WP: 1533), "Folate metabolism" (WP: 176), "antibacterial humoral response" (GO: 0019731) and "Legionellosis" (KEGG: 05134). The "humoral immune response" was linked to the N-specific proteins: Complement C3 (C3), Cathepsin G (CTSG), Neutrophil elastase (ELANE) and Keratin, type II cytoskeletal 6 A (KRT6A). "IL-17 signalling pathway" was associated with Mucin-5AC (MUC5AC) and S100-A8 (S100A8) proteins. "Vitamin B12 metabolism" and "Folate metabolism" were connected to Myeloperoxidase (MPO). Finally, the N-specific proteins, CTGS and ELANE, were associated to the "antibacterial humoral response" and C3 protein with "Legionellosis".

FE's proteome is specifically associated to "HIF1A and PPARG regulation of glycolysis" (WP: 2456) where the specific-cluster protein LDHA was detected as part of this pathway (see Table 4). The proteome of FE subgroup was also associated with "Peroxisome" (KEGG: 04146), "Central carbon metabolism in cancer" (KEGG: 05230), "DNA biosynthetic process" (GO: 0071897), "regulation of DNA biosynthetic process" (GO: 2000278), "myeloid leukocyte migration" (GO: 0097529), "leukocyte chemotaxis" (GO: 0030595), "Propanoate metabolism" (KEGG: 00640), "FBXL10 enhancement of MAP/ERK signalling in diffuse large B-cell lymphoma" (WP: 4553) and "Photodynamic therapy-induces HIF-1 survival signalling" (WP: 3614) (see Table 4).

The "Peroxisome" pathway was associated with the FE-specific proteins GSTK1 and Isocitrate dehydrogenase [NADP] (IDH1). "Central carbon metabolism in cancer" was linked with IDH1 and LDHA. "DNA biosynthetic process" was associated to Protein Niban 2 (NIBAN2) and Heterogeneous nuclear ribonucleoprotein U (HNRNPU). The "myeloid leukocyte migration" and "leukocyte chemotaxis" were both connected with CTSG and S100A8 proteins. "Propanoate metabolism" and "Photodynamic therapy-induces HIF-1 survival signalling" were linked with LDHA. Finally, "FBXL10 enhancement of MAP/ERK signalling in diffuse large B-cell lymphoma" was associated with the Histone H3.1 (H3C7).

The proteome of the F subgroup showed specific association with "Arginine and proline metabolism" (KEGG: 00330) and "Photodynamic therapy-induced NFE2L2 (NRF2) survival signalling" (WP: 3612). F group unique proteins linked to "Arginine and proline metabolism" and "Photodynamic therapy-induced NFE2L2 (NRF2) survival signalling" were Creatine kinase U-type, mitochondrial (CKMT1B), Cytosol aminopeptidase (LAP3) and Liver carboxylesterase 1 (CES1), Glutathione S-transferase P (GSTP1), respectively.

3.3.2. *Differentially expressed proteins*

Label free strategy was used for relative quantification of the identified proteins by using the NIAF values obtained from the extracted-ion chromatogram (XIC). The relative abundance of proteins simultaneously present in all three groups ($n_{proteins} = 66$ in NS, NSE and S), or in the five

Table 3
Biological Processes/Pathways Specifically Associated to the Proteome of "Non Smokers" SHS Exposed and Not Exposed.

CLUSTER NSE *versus* NS							
Biological Processes Specific of NSE[a]							
ID	**Term**	**Term PValue Corrected Bonferroni step down**	**Group PValue Corrected Bonferroni step down**	**% Associated Genes**	**Nr. Genes**	**Genes Cluster NSE**	**Genes Cluster NS**
WP:2456	**HIF1A and PPARG regulation of glycolysis**	5.09E-04	4.64E-04	37.50	3.00	**[GAPDH, LDHA, TPI1]**	**[GAPDH, TPI1]**
GO:0004602	**glutathione peroxidase activity**	4.15E-03	3.82E-03	18.75	3.00	**[GSTA1, GSTK1, PRDX5]**	**[GSTA1, PRDX5]**
KEGG:00480	**Glutathione metabolism**	1.19E-02	1.11E-02	6.90	4.00	**[GSTA1, GSTK1, IDH2, PGD]**	**[GSTA1, IDH2]**
GO:0071621	**granulocyte chemotaxis**	1.55E-02	1.49E-02	6.06	4.00	**[ANXA1, LGALS3, PPIA, PPIB]**	**[ANXA1, PPIB]**
KEGG:00640	**Propanoate metabolism**	1.63E-02	1.53E-02	9.38	3.00	**[ECHS1, LDHA, LDHB]**	**[ECHS1, LDHB]**
GO:0046496	**nicotinamide nucleotide metabolic process**	2.43E-02	2.43E-02	7.32	3.00	**[PGD, TKT, VCP]**	**[TKT, VCP]**
KEGG:05204	**Chemical carcinogenesis**	2.44E-02	2.44E-02	4.35	3.00	**[EPHX1, GSTA1, GSTK1]**	**[EPHX1, GSTA1]**
Biological Processes Specific of NS[b]							
ID	**Term**	**Term PValue Corrected with Bonferroni step down**	**Group PValue Corrected with Bonferroni step down**	**% Associated Genes**	**Nr. Genes**	**Genes Cluster NSE**	**Genes Cluster NS**
KEGG:04918	**Thyroid hormone synthesis**	1.68E-02	1.68E-02	5.33	4.00	**[ATP1A1, HSP90B1]**	**[ATP1A1, ATP1B1, HSP90B1, PDIA4]**
KEGG:04973	**Carbohydrate digestion and absorption**	2.49E-02	2.49E-02	6.38	3.00	**[ATP1A1]**	**[ATP1A1, ATP1B1, HK1]**

[a] "Non Smokers Exposed" to cigarette Second-Hand Smoke (SHS)
[b] "Non Smokers" not Exposed to SHS

subgroups ($n_{proteins}$ = 64 in N, NE, F, FE and S), were compared. Differentially abundant proteins between groups and subgroups are shown in Fig. 4 and Fig. 5, respectively.

Alcohol dehydrogenase 1 C (ADH1C), Glyceraldehyde-3-phosphate dehydrogenase (GAPDH), Elongation factor 2 (EEF2) and Triosephosphate isomerase (TPI1) were identified as being significantly higher ($p<0.05$), and Tubulin beta-4B (TUBB4B) as lower abundant ($p<0.05$) in NSE compared with NS (Fig. 4).

In comparison with S, ADH1C was higher in both NS and NSE ($p<0.05$ and $p<0.01$, respectively) (see Fig. 4**A**), whereas GAPDH and TPI1 were higher ($p<0.05$) only in NSE compared to S (Fig. 4**B** and Fig. 4**D**). The EEF2 in the NSE showed a higher abundance level compared to S group, but without statistical significance (Fig. 4**C**). The abundance level the TUBB4B between NSE and S was very similar, being, in both groups, lower than the NS (see Fig. 4**E**).

Fig. 5 shows the differentially abundant proteins among the five subgroups under study. ADH1C, GAPDH and TPI1 presented a tendency to increase in the exposed (NE, FE) *versus* non-exposed subgroups (N, F), which is in accordance to what was obtained above in the non-smoker group (see Fig. 5**A**, Fig. 5**D** and Fig. 5**G**). Three proteins, Na+, K+ -ATPase (ATP1A1), Lysozyme C (LYZ) and Serpin B3 (SERPINB3) were detected as significantly higher ($p<=0.05$) in abundance (Fig. 5**B**, Fig. 5**E** and Fig. 5**F**), while TUBB4B was significantly lower ($p<0.05$) (see Fig. 5**H**), in FE *versus* F subgroups). EEF2 was identified higher in the subgroup NE *versus* N ($p<0.05$) (Fig. 5**C**).

The absence in significant modulation of proteins in subgroups, found to be differentially expressed in groups' comparisons, may be due to sample size differences (Fig. 4 and Fig. 5**).**

3.3.3. Results verification

Shotgun MS results verification was performed by SRM assay for the elongation factor 2 (EEF2), whose expression modulation showed to be associated with SHS exposure. After manual selection of the best MS transitions, a final SRM assay was constructed with two unique peptides with seven transitions each (Table SI2).

Samples were spiked with the synthetic version of the naturally occurring peptides. After total intensity normalization, peptide integrated peak areas were compared between NE *versus* N. The two peptides behaved in the exact same way as shown in the results above (Fig. 4**C** and Fig. 5**C**), showing an increase in nasal samples from SHS exposed workers (see Fig. 6). One of the peptides was statistically significant in NE compared with N subgroup (Fig. 6**A**). SRM data obtained for EEF2 protein orthogonally confirmed the MS shotgun data.

4. Discussion

Previously we showed that non-smokers employees from a group of Lisbon restaurants with smoking free dining rooms (Legislation prior to 2015), presented higher levels of urinary cotinine and changes in their plasma proteome associated with SHS exposure at the workplace (Pacheco et al., 2013). Herein, to further investigate airway molecular events in response to SHS that could be used in health risk assessment, a comparative shotgun proteomics study was performed on the nasal airway epithelium samples from those non-smokers occupationally exposed to SHS.

In accordance with our previous data (Simões et al., 2011), the proteome of the nasal epithelium was shown to be enriched by proteins from biological processes associated with the immune protection against external microorganisms and other pathogens, drug and xenobiotics metabolism, antioxidant response to ROS and defence against inhaled oxidants and noxious compounds. These findings confirm the relevance of the nasal epithelium as a defensive barrier of the upper airways against external risk factors, and therefore, its use as airway cell model to evaluate the biological effect of environmental air pollutants, such as SHS, as we proposed here.

Indeed, by evaluating non-smoker workers exposed to SHS (NSE), their nasal epithelium showed to be particularly enriched by "glutathione peroxidase activity", "glutathione metabolism" and "HIF1A and PPARG regulation of glycolysis" pathways. Cigarette smoke induces oxidative damage to vital molecules in cells, including glutathione, a

Table 4
Biological Processes/Pathways Specifically Associated to the Proteome of "Never" and "Former" Smokers SHS Exposed and Not Exposed.

CLUSTER NE *versus* N							
Biological Processes Specific of NE[a]							
ID	**Term**	**Term PValue Corrected Bonferroni step down**	**Group PValue Corrected Bonferroni step down**	**% Associated Genes**	**Nr. Genes**	**Genes Cluster NE**	**Genes Cluster N**
GO:0035304	regulation of protein dephosphorylation	1.20E-03	1.13E-03	8.06	5.00	[HSP90AB1, HSP90B1, PPIA, YWHAB, YWHAE]	[HSP90AB1, HSP90B1, YWHAE]
KEGG:00480	Glutathione metabolism	3.21E-02	3.21E-02	5.17	3.00	[GSTK1, IDH2, PGD]	[IDH2]
Biological Processes Specific of N[b]							
ID	**Term**	**Term PValue Corrected Bonferroni step down**	**Group PValue Corrected Bonferroni step down**	**% Associated Genes**	**Nr. Genes**	**Genes Cluster NE**	**Genes Cluster N**
GO:0006959	humoral immune response	4.21E-05	4.00E-05	6.30	8.00	[BPIFA1, GAPDH, KRT1, PHB1]	[BPIFA1, C3, CTSG, ELANE, GAPDH, KRT1, KRT6A]
KEGG:04613	Neutrophil extracellular trap formation	8.71E-05	8.24E-05	4.74	9.00	[H4–16, SLC25A5, SLC25A6, VDAC1, VDAC2]	[C3, CTSG, ELANE, H4–16, MPO, SLC25A5, SLC25A6, VDAC1, VDAC2]
GO:0019730	antimicrobial humoral response	4.52E-03	4.19E-03	5.95	5.00	[BPIFA1, GAPDH]	[BPIFA1, CTSG, ELANE, GAPDH, KRT6A]
KEGG:04657	IL-17 signaling pathway	6.56E-03	6.29E-03	5.32	5.00	[HSP90AA1, HSP90AB1, HSP90B1]	[HSP90AA1, HSP90AB1, HSP90B1, MUC5AC, S100A8]
WP:1533	Vitamin B12 metabolism	3.32E-02	1.43E-02	5.66	3.00	[HBA1, HBB]	[HBA1, HBB, MPO]
WP:176	Folate metabolism	1.01E-02	1.43E-02	4.11	3.00	[HBA1, HBB]	[HBA1, HBB, MPO]
GO:0019731	antibacterial humoral response	2.82E-02	2.51E-02	6.25	3.00	[BPIFA1]	[BPIFA1, CTSG, ELANE]
KEGG:05134	Legionellosis	3.57E-02	3.57E-02	5.26	3.00	[HSPD1, VCP]	[C3, HSPD1, VCP]
CLUSTER FE *versus* F							
Biological Processes Specific of FE[c]							
ID	**Term**	**Term PValue Corrected Bonferroni step down**	**Group PValue Corrected Bonferroni step down**	**% Associated Genes**	**Nr. Genes**	**Genes Cluster FE**	**Genes Cluster F**
WP:2456	HIF1A and PPARG regulation of glycolysis	1.44E-03	1.12E-03	37.50	3.00	[GAPDH, LDHA, TPI1]	[GAPDH, TPI1]
KEGG:04146	Peroxisome	2.24E-03	1.72E-03	7.32	6.00	[GSTK1, IDH1, IDH2, PRDX1, PRDX5, SOD2]	[IDH2, PRDX1, PRDX5, SOD2]
KEGG:05230	Central carbon metabolism in cancer	9.94E-03	7.31E-03	7.14	5.00	[HK1, IDH1, IDH2, LDHA, LDHB]	[HK1, IDH2, LDHB]
GO:0071897	DNA biosynthetic process	3.03E-02	2.25E-02	4.17	6.00	[HNRNPU, HSP90AA1, HSP90AB1, NIBAN2, VCP, XRCC5]	[HSP90AA1, HSP90AB1, VCP, XRCC5]
GO:2000278	regulation of DNA biosynthetic process	3.70E-02	2.25E-02	4.67	5.00	[HNRNPU, HSP90AA1, HSP90AB1, NIBAN2, XRCC5]	[HSP90AA1, HSP90AB1, XRCC5]
GO:0097529	myeloid leukocyte migration	4.81E-02	2.36E-02	4.10	5.00	[ANXA1, CTSG, LGALS3, PPIB, S100A8]	[ANXA1, LGALS3, PPIB]
GO:0030595	leukocyte chemotaxis	2.78E-02	2.36E-02	4.35	6.00	[ANXA1, CALR, CTSG, LGALS3, PPIB, S100A8]	[ANXA1, CALR, LGALS3, PPIB]
KEGG:00640	Propanoate metabolism	4.33E-02	2.64E-02	9.38	3.00	[ECHS1, LDHA, LDHB]	[ECHS1, LDHB]
WP:4553	FBXL10 enhancement of MAP/ERK signaling in diffuse large B-cell lymphoma	4.96E-02	3.10E-02	7.89	3.00	[H3–3A, H3C13, H3C7]	[H3–3A, H3C13]
WP:3614	Photodynamic therapy-induced HIF-1 survival signaling	4.88E-02	3.16E-02	8.11	3.00	[HK1, LDHA, PGK1]	[HK1, PGK1]
Biological Processes Specific of F[d]							
ID	**Term**	**Term PValue Corrected Bonferroni step down**	**Group PValue Corrected Bonferroni step down**	**% Associated Genes**	**Nr. Genes**	**Genes Cluster FE**	**Genes Cluster F**

(*continued on next page*)

Table 4 (*continued*)

Biological Processes Specific of F[d]							
ID	**Term**	**Term PValue Corrected Bonferroni step down**	**Group PValue Corrected Bonferroni step down**	**% Associated Genes**	**Nr. Genes**	**Genes Cluster FE**	**Genes Cluster F**
KEGG:00330	**Arginine and proline metabolism**	2.60E-02	1.90E-02	7.84	4.00	**[ALDH2, GOT2]**	**[ALDH2, CKMT1B, GOT2, LAP3]**
WP:3612	**Photodynamic therapy-induced NFE2L2 (NRF2) survival signaling**	2.90E-02	2.17E-02	12.50	3.00	**[EPHX1]**	**[CES1, EPHX1, GSTP1]**

[a] "Never Smokers Exposed" to cigarette Second-Hand Smoke (SHS)
[b] "Never Smokers" not Exposed to SHS
[c] "Former Smokers Exposed" to SHS
[d] "Former Smokers" not Exposed to SHS

power antioxidant, which has a role in detoxification of toxins, xenobiotics, and drugs (Dalle-Donne et al., 2020). Interestingly, "glutathione metabolism" was enriched in both NSE group and NE subgroup but not in FE subgroup, suggesting an exposure adaptation response towards SHS detoxification only in subjects that never smoked. However, further studies will be needed to confirm this assumption.

The transcription factor hypoxia-inducible factor-1α (HIF1A) is known to regulate a number of genes in response to low oxygen or hypoxia and various other internal and external factors, including toxic and xenobiotic inflammatory substances such as cigarette smoke (Aschner et al., 2023). Increased expression of HIF-target genes affects numeral physiological responses like glycolytic metabolism, cell death and angiogenesis (Kierans and Taylor, 2021). Interestingly, two key glycolytic proteins, GADPH and TPI1, whose genes transcriptions are regulated by several transcription factors, including HIF1A (Higashimura et al., 2011), were found significantly up-regulated in NSE group, supporting the proteome enrichment with "HF1A and PPARG regulation glycolysis" in non-smoker subjects exposed to SHS.

Chronic exposure of non-malignant oesophageal epithelial cells to mainstream or sidestream smoke extract mimicking SHS, showed to cause modifications in cell phenotype, leading to the acquisition of tumorigenic characteristics associated with increased expression of glycolytic pathway genes to the detrimental of mitochondrial gene expression (Kim et al., 2010). However, mouse exposure to cigarette smoke for a short-term period led to a decrease in GAPDH expression, resulting in a switch of glycolysis flux to pentose phosphate pathway (Agarwal et al., 2012). Overexpression of GAPDH protein has been linked with cancer risk, namely lung cancer with a poor prognosis (Sirover, 2018), and TPI1 is also a potential biomarker for progression of some types of cancer (Pekel and Ari, 2020).

In our study, the detected up-regulation of GAPDH and TPI1 in NSE compared with NS may be a consequence of a longer response to SHS-induced oxidative stress or hypoxia in the workplace.

A significantly higher expression of ADH1C was observed in the nasal epithelium from NSE, and also in NE and FE subgroups, although without statistical significance. In contrast, a decrease of this enzyme was identified in S group compared with all non-smoker groups or subgroups exposed and non-exposed to SHS. ADH1C is the gamma subunit of the Class I alcohol dehydrogenase family that plays a critical role in ethanol oxidation and metabolism of endogenous substrates, such as retinol, fatty acids, steroids, and dopamine (Cui and Li, 2018). Polymorphisms in ADH1C gene may contribute to increased cancer risk, including squamous cell carcinoma of the head and neck associated with alcohol and tobacco smoking (Peters et al., 2005). Overexpression of ADH1C is correlated with a better prognosis of non-small cell lung cancer and colon cancer (Li et al., 2022), which are pathologies linked with cigarette smoke (Giovannucci and Martinez, 1996; Hecht, 1999). Further studies are needed to better understand the functional impact of ADH1C in the context of SHS exposure and associated cancer pathologies.

EEF2, a regulator of protein synthesis in genotoxic stress (Kruiswijk et al., 2012), was found up-regulated in NSE group and NE, FE subgroups, although with no significant statistical difference in the latter. Overexpression of EEF2 has been correlated with cancer cell progression and recurrence (Oji et al., 2014). It has been linked to lung adenocarcinoma, head and neck and lung squamous cell carcinomas (C. Y. Chen et al., 2011; Song et al., 2016).

Cigarette smoke-induced tubulin-microtubule dysregulation is correlated with tobacco smoke associated dysfunctions (e.g., impairment of ciliated cells), which, ultimately, result in cell apoptosis and tissue damage (Leopold et al., 2009; Simet et al., 2010). TUBB4B, a tubulin family member reported as essential for ciliary axonemes construction and regulation in the respiratory epithelium, was observed significantly down-regulated in NSE group, especially in FE compared with F. Compared to S group, TUBB4B was statistically up-regulated in F but not FE subgroups, suggesting an active cilia recovery process in F following smoking abstinence. Overexpression of TUBB4B is associated with hepatocellular carcinoma (Uhlen et al., 2017; Yang et al., 2023), while its down-regulation has been shown to play a role in colon cancer metastasis initiation (Sobierajska et al., 2019).

Compared with NE, the nasal proteome of FE was enriched with a higher number of biological processes and pathways, such as "Peroxisome", "HIF1A and PPARG regulation of glycolysis", "Central carbon metabolism in cancer", the "DNA biosynthetic process", "Regulation of DNA biosynthetic process" and "Myeloid leucocyte migration", among others. "Peroxisome" pathway refers to the cellular organelle that is critical in fatty acid oxidation, ether phospholipid synthesis and free radical detoxification (hydrogen peroxide (H_2O_2) metabolism). GSTK1, related with xenobiotic detoxification, and IDH1, involved in the peroxisomeś NADPH regeneration (Chandel, 2021), were two of the FE-specific proteins associated with this pathway. "HIF1A and PPARG regulation of glycolysis" and "Central carbon metabolism in cancer" pathways are associated with the Warburg effect where, under aerobic conditions, cells with high proliferative index (e.g., cancerous cells) reprogram glycolysis metabolism needed for cell growth and multiplication (Chandel, 2021). HNRNPU and NIBAN2 FE-specific proteins, linked to "DNA biosynthetic process", present functions in the mitotic cell progression and apoptosis suppression, respectively (S. Chen et al., 2011; Ma et al., 2011). "Myeloid leucocyte migration" process, was found to be associated with S100-A8 (gene S100A8), a protein that can induce neutrophil chemotaxis and adhesion, and Cathepsin G (CTSG), a protein presenting immunomodulating proprieties (Patel, 2017). Indeed, cigarette smoking exposure can promote the increase of leukocyte infiltration in affected tissues, leading to an increase in neutrophils and macrophages, which may amplify cigarette smoking-induced inflammation and compromise immune response (Jaspers, 2014). All these data suggest that FE nasal airways proteome is significantly enriched with proteins from biological processes to counteract SHS-derived xenobiotic toxicity and oxidative stress, leading to metabolic reprogramming to influence cell fate, inflammation and immune

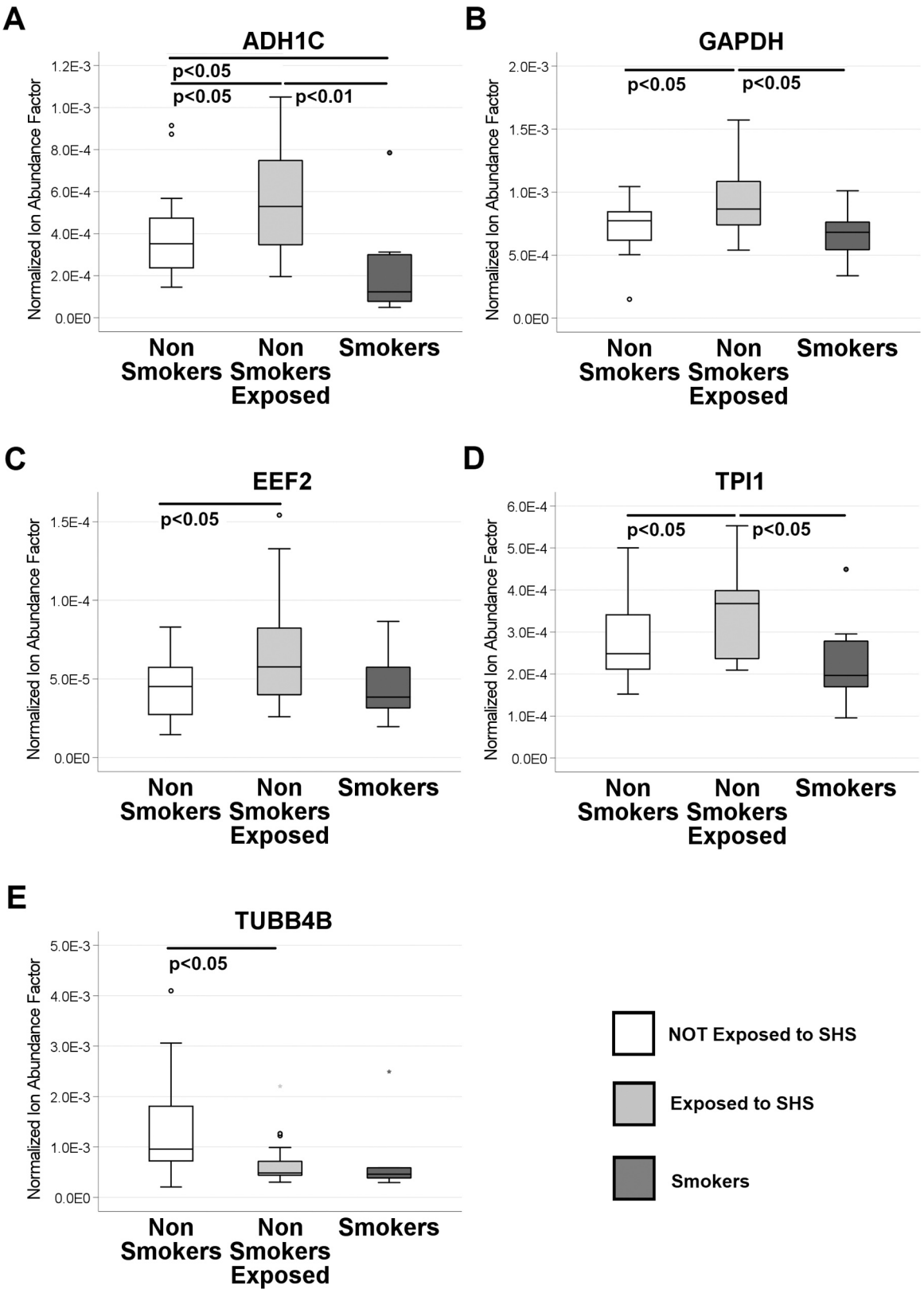

Fig. 4. Differentially abundant proteins between groups: Non-Smokers Exposed and Non-Smokers not exposed to SHS and Smokers. (A) Alcohol dehydrogenase 1 C (**ADH1C**), (B) Glyceraldehyde-3-phosphate dehydrogenase (**GAPDH**), (C) Elongation factor 2 (**EEF2**), (D) Triosephosphate isomerase (**TPI1**) and (E) Tubulin beta-4B chain (**TUBB4B**). A nonparametric independent-samples Mann-Whitney U test (α=0.05) was applied. Box plots show the median and interquartile values.

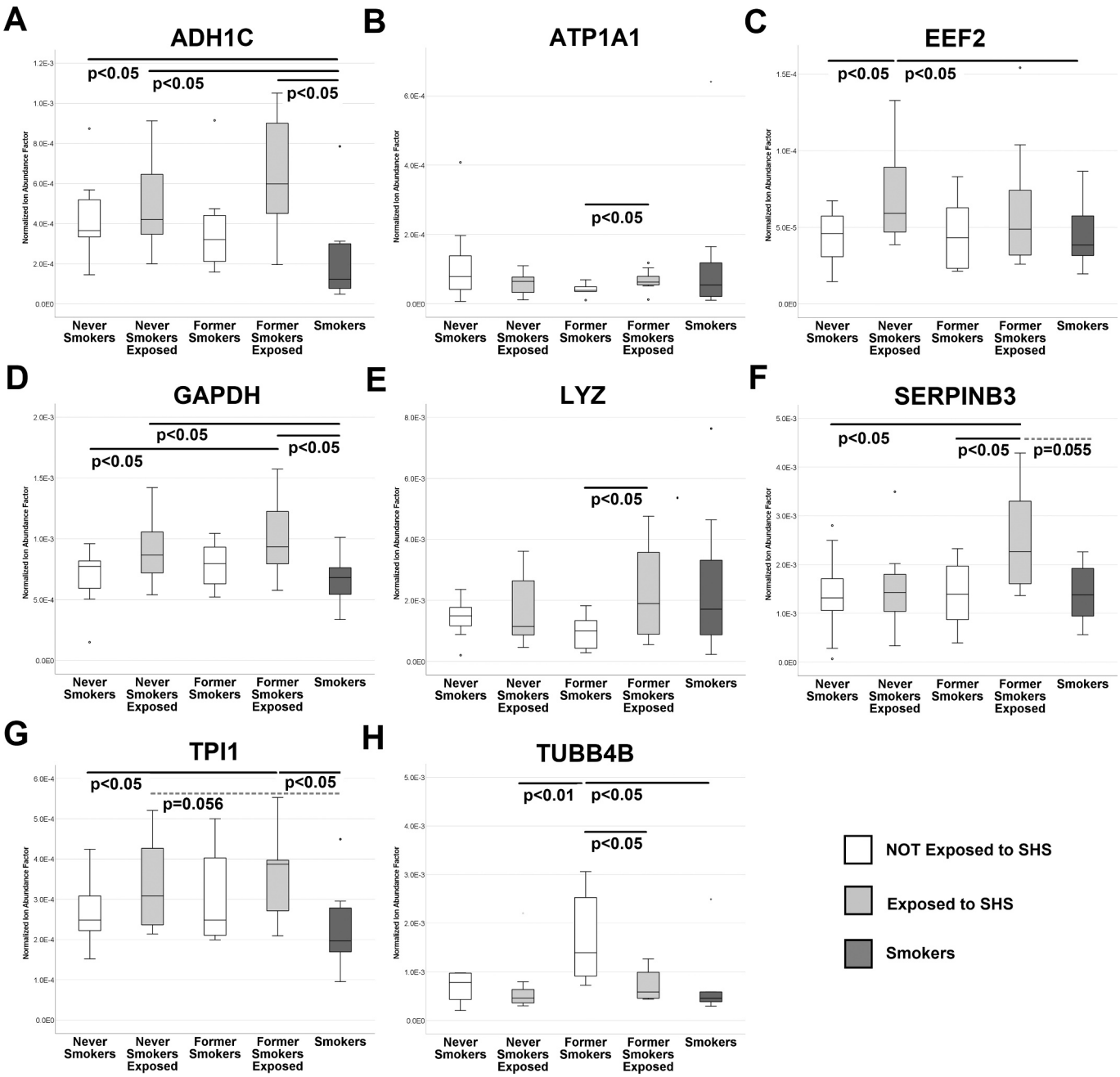

Fig. 5. Differentially abundant proteins between subgroups: Never Smokers Exposed, Former Smokers Exposed, Never Smokers and Former Smokers not exposed to SHS and Smokers. (A) Alcohol dehydrogenase 1 C (**ADH1C**), (B) Sodium/potassium-transporting ATPase subunit alpha-1 (**ATP1A1**), (C) Elongation factor 2 (**EEF2**), (D) Glyceraldehyde-3-phosphate dehydrogenase (**GAPDH**), Lysozyme C (**LYZ**), (F) Serpin B3 (**SERPINB3**), (G) Triosephosphate isomerase (**TPI1**) and (H) Tubulin beta-4B chain (**TUBB4B**). A nonparametric independent-samples Mann-Whitney U test (α=0.05) was applied. Box plots show the median and interquartile values.

response.

In FE subgroup, Serpin B3 (SERPINB3), a serine protease inhibitor, was also found specifically up-regulated. This protein was first detected in cervical squamous cell carcinoma (Kato and Torigoe, 1977) and later associated to different types of cancer development and progression, including lung cancer (Sun et al., 2017; Turato and Pontisso, 2015). Evidence points to Serpin B3 as an oncoprotein capable of promoting the epithelial-mesenchymal transition and positive regulation of c-Myc gene (Sun et al., 2017). Serpin B3 is able to inhibit the apoptotic pathway, promoting cell survival (Katagiri et al., 2006; Lauko et al., 2022; Ullman et al., 2011). In mouse model, the overexpression of Serpin B3 helps epithelial proliferation and leads to lung fibrosis (Lunardi et al., 2011). A higher expression of this protein has also been detected in respiratory chronic inflammatory conditions, such as asthma and COPD (Ray et al., 2005). Actually, patients with COPD, presented elevated expression of Serpin B3 associated with smoking (Franciosi et al., 2014).

These data lead us to hypothesize that chronic exposure to SHS may lead to Serpin B3-induced cell death inhibition and inflammatory modulation in healthy former-smoker airways exposed. This particular response may be associated with previous irreversible effect of tobacco smoking habits. Former smokers exposed to SHS may have an increased risk for chronic inflammatory conditions such as asthma and COPD compared with former smokers not exposed.

A member of the Na+/K+-ATPase sodium pump, ATP1A1, showed

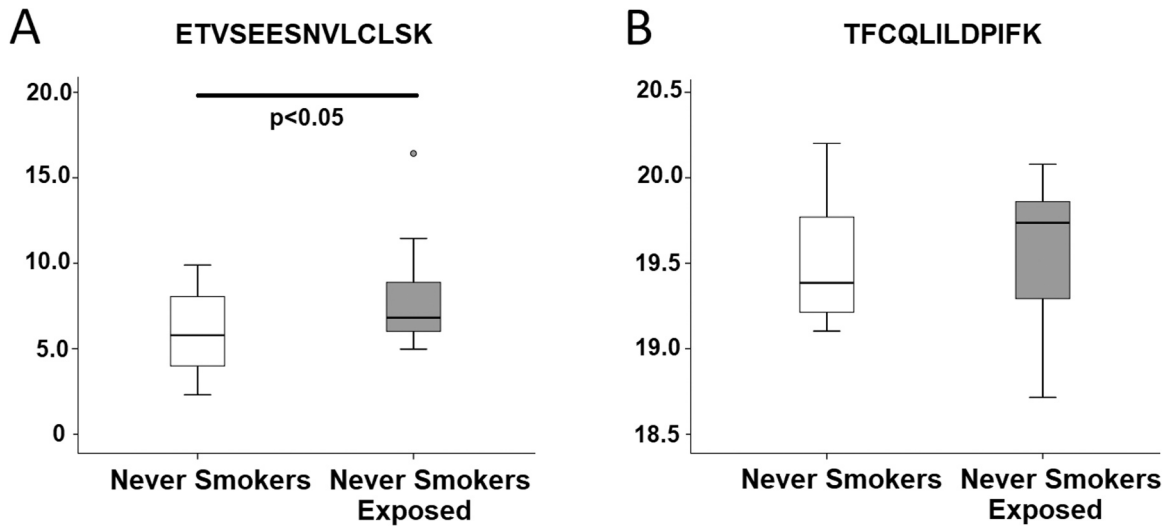

Fig. 6. Selected Reaction Monitoring (SRM) assay verification. Box plots comparing Elongation factor 2 (gene EEF2) peptide integrated peaks, between Never-Smokers Exposed and not exposed to Second hand Smoke (SHS) at the workplace. Normal distributed data was analysed with two-sided Student's t test.

up-regulated in FE compared with F subgroup. Cigarette smoke is associated with decreased Na+/K+-ATPase function, being down-regulated in lung cancer (Huynh et al., 2012). ATP1A1 decrease has also been related to a reduction of proliferation and migration of hepatic carcinoma cells, leading to cell apoptosis and reducing tumorigenicity *in vivo* (Feng et al., 2021). Nonetheless, the expression of this protein has also been described up-regulated in liver cancer and glioma (Xu et al., 2010; Zhuang et al., 2015). How changes in ATP1A1 protein expression occur in different tissues and tumours, and how this expression may contribute to disease progression and outcome, requires further investigation.

Lysozyme C (LYZ) was observed at a higher abundance in FE subgroup. Lysozymes are secreted in several organs and secretory fluids, namely in the mucosal surface. Changes in LYZ expression are associated with risk of upper respiratory tract infection (Hanstock et al., 2019). LYZ is suspected to play a role in the ability of the epithelium to recover from injury, since it has been shown to promote ischemic wound healing by improving angiogenesis and inflammation (Li et al., 2021). Knowing that all subjects were healthy at the time of sample collection, the high levels of LYZ in FE may be a protective response against SHS.

Although Smokers (S) were not the focus of our study, the expression level of the differential proteins identified in the different groups, did not show changes in S compared with Non-smokers (NS) control, except ADH1A, which showed down-regulated in S compared with NS. In the subgroups, TUBB4B revealed to be down-regulated in S when compared with the F control. These results suggest that a continuous acute response involving these proteins may be taking place in non-smokers to counteract the harmful effects of long exposure to SHS, whilst in smokers, long-term active smoking may deactivate this protective acute response, leading to an adaptive response.

4.1. Study Limitations

The sample size in each group was less than 30, which was overcome by applying more robust nonparametric statistical tests. The absence of technical replicates led to an increase in the restriction criteria of the MS identification to face the uncertainty associated with the LC-MS/MS technology, which resulted in a smaller number of identified proteins. However, the identification and quantification of these proteins were obtained with high certainty and confidence. Due to sample quantity limitation, one protein was submitted to verification by an orthogonal methodology (SRM).

This is a transversal study attempting to find protein profiles in airway epithelia associated with occupational SHS exposure. Since SHS-related diseases/pathologies are time dependent a longitudinal study with several year-follow up would provide a broader and more realistic data associated with SHS risk events. Nevertheless, the data presented in this study by evaluating nasal airway proteome from healthy (never and former) non-smoker subjects exposed to SHS at the workplace, opens new insights into SHS exposure effects, that could be useful in future follow-up studies.

5. Conclusions

The present proteomic study, by identifying biological pathways associated with the role of the nasal epithelium as a protective barrier against internal and external biological or environmental factors, confirms the importance and value of this tissue in the biological assessment of the effect of occupational chronic exposure to SHS in healthy non-smokers.

HIF1α-glycolytic targets, such as GAPDH and TPI1, and proteins related to toxin detoxification, xenobiotic metabolism, genotoxic response, cell proliferation and differentiation (e.g., ADH1C, EFF2, TUBB4B) that could lead to cancer pathology associated with tobacco smoke, showed a significant modulation in non-smoker nasal airway SHS-exposed.

In never smoker exposed nasal epithelia, the glutathione synthesis related to antioxidant and detoxification protective activity, and the EEF2-induced protein synthesis in response to genotoxic stress, were highly enriched and activated, respectively.

Biological processes related to metabolic reprogramming and modulation of cell proliferation, inflammation, differentiation and suppression of apoptosis were shown to be particularly activated in nasal airways of former smokers exposed in response to SHS derived oxidative-stress and xenobiotic toxicity. Former smokers exposed to SHS may have an increased risk for chronic inflammatory conditions such as asthma and COPD related to Serpin B3 up-regulation.

Future studies integrating proteomics and metabolomics might provide further validation and new insights into the complex biological pathways underlying upper airway response to SHS that may lead to respiratory and/or cancer diseases development. Validated proteins may be high susceptibility/risk biomarkers for respiratory disorders development in healthy non-smokers, in particular, former smokers chronically exposed to SHS.

Funding

This work was supported by the Calouste Gulbenkian Foundation, Portuguese Central Administration of Nacional Health System, the Portuguese Rede Nacional de Espectrometria de Massa, the National Institute of Health Doctor Ricardo Jorge, and the Centre for Toxicogenomics and Human Health – ToxOmics from NOVA Medical School-FCM, UNL. SN and SP were granted with PhD fellowships from Portuguese Fundação para a Ciência e a Tecnologia.

CRediT authorship contribution statement

Fátima Vaz: Project administration, Methodology, Investigation, Data curation. **Peter James:** Supervision, Resources. **Tânia Simões:** Investigation, Funding acquisition, Conceptualization. **Deborah Penque:** Writing – review & editing, Supervision, Funding acquisition, Conceptualization. **Sofia Neves:** Writing – original draft, Methodology, Investigation, Formal analysis, Data curation. **Solange Pacheco:** Validation, Methodology, Investigation, Data curation.

Declaration of Competing Interest

The authors declare that they have no known competing financial interests or personal relationships that could have appeared to influence the work reported in this paper.

Data Availability

Data will be made available on request.

Acknowledgements

We express our gratitude to all restaurants and their workers, who voluntarily participated in this study. To Professor Paulo C. Carvalho and Marlon D.M. Santos for their support in the "PatternLab for Proteomics" software interpretation. To Nuno Charro for helping in the restaurant́s recruitment process, and Joana Saraiva for helping in English text review and editing.

This work was supported by the Calouste Gulbenkian Foundation, Portuguese Central Administration of National Health System, the Portuguese Rede Nacional de Espectrometria de Massa, the National Institute of Health Dr Ricardo Jorge, and the Centre for Toxicogenomics and Human Health – ToxOmics from NOVA Medical School-FCM, UNL. SN and SP were granted with PhD fellowships from Portuguese Fundação para a Ciência e a Tecnologia.

Ethics

The study was approved by the National Institute of Health Doctor Ricardo Jorge's Ethics Committee.

Consent to participate

Informed consent was obtained from all the individuals/workers recruited for this work.

Appendix A. Supporting information

Supplementary data associated with this article can be found in the online version at doi:10.1016/j.etap.2024.104459.

References

Agarwal, A.R., Zhao, L., Sancheti, H., Sundar, I.K., Rahman, I., Cadenas, E., 2012. Short-term cigarette smoke exposure induces reversible changes in energy metabolism and cellular redox status independent of inflammatory responses in mouse lungs. Am. J. Physiol. Lung Cell Mol. Physiol. 303, 889–898. https://doi.org/10.1152/ajplung.00219.2012.

Aschner, M., Skalny, A.V., Lu, R., Santamaria, A., Zhou, J.C., Ke, T., Karganov, M.Y., Tsatsakis, A., Golokhvast, K.S., Bowman, A.B., Tinkov, A.A., 2023. The role of hypoxia-inducible factor 1 alpha (HIF-1α) modulation in heavy metal toxicity. Arch. Toxicol. 97, 1299–1318. https://doi.org/10.1007/s00204-023-03483-7.

Carreras, G., Lugo, A., Gallus, S., Cortini, B., Fernández, E., López, M.J., Soriano, J.B., López-Nicolás, A., Semple, S., Gorini, G., Castellano, Y., Fu, M., Ballbè, M., Amalia, B., Tigova, O., Continente, X., Arechavala, T., Henderson, E., Liu, X., Bosetti, C., Davoli, E., Colombo, P., O'Donnell, R., Dobson, R., Clancy, L., Keogan, S., Byrne, H., Behrakis, P., Tzortzi, A., Vardavas, C., Vyzikidou, V.K., Bakellas, G., Mattiampa, G., Boffi, R., Ruprecht, A., De Marco, C., Borgini, A., Veronese, C., Bertoldi, M., Tittarelli, A., Verdi, S., Chellini, E., Trapero-Bertran, M., Guerrero, D.C., Radu-Loghin, C., Nguyen, D., Starchenko, P., Ancochea, J., Alonso, T., Pastor, M.T., Erro, M., Roca, A., Pérez, P., 2019. Burden of disease attributable to second-hand smoke exposure: A systematic review. Prev. Med (Balt.). https://doi.org/10.1016/j.ypmed.2019.105833.

Carvalho, P.C., Fischer, J.S.G., Xu, T., Yates 3rd, J.R., Barbosa, V.C., 2013. PatternLab: from mass spectra to label-free differential shotgun proteomics. Curr. Protoc. Bioinforma. 13, 13. 19. 1-13. 19. 18. https://doi.org/10.1002/0471250953.bi1319s40.

Carvalho, P.C., Lima, D.B., Leprevost, F.V., Santos, M.D.M., Fischer, J.S.G., Aquino, P.F., Moresco, J.J., Yates, J.R., Barbosa, V.C., 2016. Integrated analysis of shotgun proteomic data with PatternLab for proteomics 4.0. Nat. Protoc. 11, 102–117. https://doi.org/10.1038/nprot.2015.133.

Chandel, N.S., 2021. Glycolysis. Cold Spring Harb. Perspect. Biol. 13, 1–11. https://doi.org/10.1101/CSHPERSPECT.A040535.

Chawade, A., Alexandersson, E., Levander, F., 2014. Normalyzer: A tool for rapid evaluation of normalization methods for omics data sets. J. Proteome Res 13, 3114–3120. https://doi.org/10.1021/pr401264n.

Chen, S., Evan, H.G., Evans, D.R., 2011. FAM129B/MINERVA, a novel adherens junction-associated protein, suppresses apoptosis in HeLa cells. J. Biol. Chem. 286, 10201–10209. https://doi.org/10.1074/jbc.M110.175273.

Chen, C.Y., Fang, H.Y., Chiou, S.H., Yi, S.E., Huang, C.Y., Chiang, S.F., Chang, H.W., Lin, T.Y., Chiang, I.P., Chow, K.C., 2011. Sumoylation of eukaryotic elongation factor 2 is vital for protein stability and anti-apoptotic activity in lung adenocarcinoma cells. Cancer Sci. 102, 1582–1589. https://doi.org/10.1111/j.1349-7006.2011.01975.x.

Consortium, T.U., 2023. UniProt: the Universal Protein Knowledgebase in 2023, 51, 523–531. https://doi.org/10.1093/nar/gkac1052.

Cui, J., Li, C., 2018. Regulation of Xenobiotic Metabolism in the Liver. In: McQueen, C.A. (Ed.), COMPREHENSIVE TOXICOLOGY. Elsevier, Waltham, pp. 173–174.

Dalle-Donne, I., Garavaglia, M.L., Colombo, G., Astori, E., Lionetti, M.C., La Porta, C.A. M., Santucci, A., Rossi, R., Giustarini, D., Milzani, A., 2020. Cigarette smoke and glutathione: Focus on in vitro cell models. Toxicol. Vitr. https://doi.org/10.1016/j.tiv.2020.104818.

Feng, X.Y., Zhao, W., Yao, Z., Wei, N.Y., Shi, A.H., Chen, W.H., 2021. Downregulation of ATP1A1 Expression by Panax notoginseng (Burk.) F.H. Chen Saponins: A Potential Mechanism of Antitumor Effects in HepG2 Cells and In Vivo. Front Pharm. 12 https://doi.org/10.3389/fphar.2021.720368.

Franciosi, L., Postma, D.S., Van Den Berge, M., Govorukhina, N., Horvatovich, P.L., Fusetti, F., Poolman, B., Lodewijk, M.E., Timens, W., Bischoff, R., Ten Hacken, N.H. T., 2014. Susceptibility to COPD: Differential proteomic profiling after acute smoking. PLoS One 9, 3–11. https://doi.org/10.1371/journal.pone.0102037.

Giovannucci, E., Martinez, M.E., 1996. Tobacco, colorectal cancer, and adenomas: a review of the evidence. J. Natl. Cancer Inst. 88, 1717–1747. https://doi.org/10.1093/jnci/88.23.1717.

Gower, A.C., Steiling, K., Ii, J.F.B., Lenburg, M.E., Spira, A., 2011. Transcriptomic Studies of the Airway Field of Injury Associated with Smoking-Related Lung Disease. Proc. Am. Thorac. Soc. 8, 173–179. https://doi.org/10.1513/pats.201011-066MS.

Hanstock, H.G., Edwards, J.P., Walsh, N.P., 2019. Tear lactoferrin and lysozyme as clinically relevant biomarkers of mucosal immune competence. Front Immunol. 10, 1–11. https://doi.org/10.3389/fimmu.2019.01178.

Hecht, S.S., 1999. Tobacco Smoke Carcinogens and Lung Cancer. J. Nac. Cancer Inst. 91, 1194–1210. https://doi.org/10.1093/jnci/91.14.1194.

Higashimura, Y., Nakajima, Y., Yamaji, R., Harada, N., Shibasaki, F., Nakano, Y., Inui, H., 2011. Up-regulation of glyceraldehyde-3-phosphate dehydrogenase gene expression by HIF-1 activity depending on Sp1 in hypoxic breast cancer cells. Arch. Biochem Biophys. 509, 1–8. https://doi.org/10.1016/j.abb.2011.02.011.

Huynh, T.P., Mah, V., Sampson, V.B., Chia, D., Fishbein, M.C., Horvath, S., Alavi, M., Wu, D.C., Harper, J., Sarafian, T., Dubinett, S.M., Langhans, S.A., Goodglick, L., Rajasekaran, A.K., 2012. Na,K-ATPase is a target of cigarette smoke and reduced expression predicts poor patient outcome of smokers with lung cancer. Am. J. Physiol. Lung Cell Mol. Physiol. 302, 1150–1158. https://doi.org/10.1152/ajplung.00384.2010.

Jaspers, I., 2014. Cigarette smoke effects on innate immune mechanisms in the nasal mucosa: Potential effects on the microbiome, in. Ann. Am. Thorac. Soc. https://doi.org/10.1513/AnnalsATS.201306-154MG.

Katagiri, C., Nakanishi, J., Kadoya, K., Hibino, T., 2006. Serpin squamous cell carcinoma antigen inhibits UV-induced apoptosis via suppression of c-JUN NH2-terminal kinase. J. Cell Biol. 172, 983–990. https://doi.org/10.1083/jcb.200508064.

Kato, H., Torigoe, T., 1977. Radioimmunoassay for tumor antigen of human cervical squamous cell carcinoma. Cancer 40, 1621–1628. https://doi.org/10.1002/1097-0142(197710)40:4<1621::aid-cncr2820400435>3.0.co;2-i.

Kierans, S.J., Taylor, C.T., 2021. Regulation of glycolysis by the hypoxia-inducible factor (HIF): implications for cellular physiology. J. Physiol. https://doi.org/10.1113/JP280572.

Kim, M.S., Huang, Y., Lee, J., Zhong, X., Jiang, W.W., Ratovitski, E.A., Sidransky, D., 2010. Cellular transformation by cigarette smoke extract involves alteration of glycolysis and mitochondrial function in esophageal epithelial cells. Int J. Cancer 127, 269–281. https://doi.org/10.1002/ijc.25057.

Kruiswijk, F., Yuniati, L., Magliozzi, R., TY, L., Lim, R., Bolder, R., Mohammed, S., Proud, C., Heck, A., Pagano, M., Guardavaccaro, D., 2012. Coupled activation and degradation of eEF2K regulates protein synthesis in response to genotoxic stress. Sci. Signal 5, ra40 https://doi.org/doi:10.1126/scisignal.2002718.

Lauko, A., Volovetz, J., Turaga, S.M., Bayik, D., Silver, D.J., Mitchell, K., Mulkearns-Hubert, E.E., Watson, D.C., Desai, K., Midha, M., Hao, J., McCortney, K., Steffens, A., Naik, U., Ahluwalia, M.S., Bao, S., Horbinski, C., Yu, J.S., Lathia, J.D., 2022. SerpinB3 drives cancer stem cell survival in glioblastoma. Cell Rep. 40 https://doi.org/10.1016/j.celrep.2022.111348.

Leopold, P.L., O'Mahony, M.J., Julie Lian, X., Tilley, A.E., Harvey, B.G., Crystal, R.G., 2009. Smoking is associated with shortened airway Cilia. PLoS One 4. https://doi.org/10.1371/journal.pone.0008157.

Li, W., Jiang, Y.X., Chen, Q.Y., Wang, G.G., 2021. Recombinant fusion protein by lysozyme and antibacterial peptide enhances ischemic wound healing via angiogenesis and reduction of inflammation in diabetic db/db mice. PeerJ 9. https://doi.org/10.7717/peerj.11256.

Li, S., Yang, H., Li, W., Liu, J. yi, Ren, L. wen, Yang, Y. hui, Ge, B. bin, Zhang, Y. zhi, Fu, W. qi, Zheng, X. jin, Du, G. hua, Wang, J.H., 2022. ADH1C inhibits progression of colorectal cancer through the ADH1C/PHGDH /PSAT1/serine metabolic pathway. Acta Pharm. Sin. 43, 2709–2722. https://doi.org/10.1038/s41401-022-00894-7.

Lunardi, F., Villano, G., Perissinotto, E., Agostini, C., Rea, F., Gnoato, M., Bradaschia, A., Valente, M., Pontisso, P., Calabrese, F., 2011. Overexpression of SERPIN B3 promotes epithelial proliferation and lung fibrosis in mice. Lab. Investig. 91, 945–954. https://doi.org/10.1038/labinvest.2011.1.

Ma, N., Matsunaga, S., Morimoto, A., Sakashita, G., Urano, T., Uchiyama, S., Fukui, K., 2011. The nuclear scaffold protein SAF-A is required for kinetochore-microtubule attachment and contributes to the targeting of Aurora-A to mitotic spindles. J. Cell Sci. 124, 394–404. https://doi.org/10.1242/jcs.063347.

MacLean, B., Tomazela, D.M., Shulman, N., Chambers, M., Finney, G.L., Frewen, B., Kern, R., Tabb, D.L., Liebler, D.C., MacCoss, M.J., 2010. Skyline: An open source document editor for creating and analyzing targeted proteomics experiments. Bioinformatics 26, 966–968. https://doi.org/10.1093/bioinformatics/btq054.

Marques, H., Cruz-Vicente, P., Rosado, T., Barroso, M., Passarinha, L.A., Gallardo, E., 2021. Recent developments in the determination of biomarkers of tobacco smoke exposure in biological specimens: A review. Int J. Environ. Res Public Health. https://doi.org/10.3390/ijerph18041768.

Mlecnik, B., Galon, J., Bindea, G., 2018. Comprehensive functional analysis of large lists of genes and proteins. J. Proteom. 171, 2–10. https://doi.org/10.1016/j.jprot.2017.03.016.

Oji, Y., Tatsumi, N., Fukuda, M., Nakatsuka, S.I., Aoyagi, S., Hirata, E., Nanchi, I., Fujiki, F., Nakajima, H., Yamamoto, Y., Shibata, S., Nakamura, M., Hasegawa, K., Takagi, S., Fukuda, I., Hoshikawa, T., Murakami, Y., Mori, M., Inoue, M., Naka, T., Tomonaga, T., Shimizu, Y., Nakagawa, M., Hasegawa, J., Nezu, R., Inohara, H., Izumoto, S., Nonomura, N., Yoshimine, T., Okumura, M., Morii, E., Maeda, H., Nishida, S., Hosen, N., Tsuboi, A., Oka, Y., Sugiyama, H., 2014. The translation elongation factor eEF2 is a novel tumor-associated antigen overexpressed in various types of cancers. Int J. Oncol. 44, 1461–1469. https://doi.org/10.3892/ijo.2014.2318.

Pacheco, S.A., Aguiar, F., Ruivo, P., Proença, M.C., Sekera, M., Penque, D., Simões, T., 2012. Occupational exposure to environmental tobacco smoke: A study in Lisbon restaurants. : J. Toxicol. Environ. Health - Part A: Curr. Issues 857–866. https://doi.org/10.1080/15287394.2012.690690.

Pacheco, S.A., Torres, V.M., Louro, H., Gomes, F., Lopes, C., Marçal, N., Fragoso, E., Martins, C., Oliveira, C.L., Hagenfeldt, M., Bugalho-Almeida, A., Penque, D., Simões, T., 2013. Effects of occupational exposure to tobacco smoke: Is there a link between environmental exposure and disease? J. Toxicol. Environ. Health - Part A: Curr. Issues 76, 311–327. https://doi.org/10.1080/15287394.2013.757269.

Patel, S., 2017. A critical review on serine protease: Key immune manipulator and pathology mediator. Allergol. Immunopathol. (Madr. https://doi.org/10.1016/j.aller.2016.10.011.

Pekel, G., Ari, F., 2020. Therapeutic Targeting of Cancer Metabolism with Triosephosphate Isomerase. Chem. Biodivers. 17 https://doi.org/10.1002/cbdv.202000012.

Penque, D., Mendes, F., Beck, S., Farinha, C., Pacheco, P., Nogueira, P., Lavinha, J., Malhó, R., Amaral, M.D., 2000. Cystic fibrosis F508del patients have apically localized CFTR in a reduced number of airway cells. Lab. Investig. 80, 857–868. https://doi.org/10.1038/labinvest.3780090.

Peters, E.S., Mcclean, M.D., Liu, M., Eisen, E.A., Mueller, N., Kelsey, K.T., 2005. The ADH1C Polymorphism Modifies the Risk of Squamous Cell Carcinoma of the Head and Neck Associated with Alcohol and Tobacco Use. Cancer Epidemiol. Biomark. Prev. 14, 476–482. https://doi.org/10.1158/1055-9965.EPI-04-0431.

Ray, R., Choi, M., Zhang, Z., Silverman, G.A., Askew, D., Mukherjee, A.B., 2005. Uteroglobin suppresses SCCA gene expression associated with allergic asthma. J. Biol. Chem. 280, 9761–9764. https://doi.org/10.1074/jbc.C400581200.

Simet, S.M., Sisson, J.H., Pavlik, J.A., DeVasure, J.M., Boyer, C., Liu, X., Kawasaki, S., Sharp, J.G., Rennard, S.I., Wyatt, T.A., 2010. Long-term cigarette smoke exposure in a mouse model of ciliated epithelial cell function. Am. J. Respir. Cell Mol. Biol. 43, 635–640. https://doi.org/10.1165/rcmb.2009-0297OC.

Simões, T., Charro, N., Blonder, J., Faria, D., Couto, F.M., Chan, K.C., Waybright, T., Isaaq, H.J., Veenstra, T.D., Penque, D., 2011. Molecular profiling of the human nasal epithelium: A proteomics approach. J. Proteom. 75, 56–69. https://doi.org/10.1016/j.jprot.2011.05.012.

Sirover, M.A., 2018. Pleiotropic effects of moonlighting glyceraldehyde-3-phosphate dehydrogenase (GAPDH) in cancer progression, invasiveness, and metastases. Cancer Metastas-.-. Rev. https://doi.org/10.1007/s10555-018-9764-7.

Sobierajska, K., Ciszewski, W.M., Wawro, M.E., Wieczorek-szukała, K., Boncela, J., Papiewska-Pajak, I., Niewiarowska, J., Kowalska, M.A., 2019. TUBB4B downregulation is critical for increasing migration of metastatic colon cancer cells. Cells 8. https://doi.org/10.3390/cells8080810.

Song, Y., Sun, B., Hao, L.H., Hu, J., Du, S., Zhou, X., Zhang, L.Y., Liu, L., Gong, L.L., Chi, X.M., Liu, Q., Shao, S.J., 2016. Elevated eukaryotic elongation factor 2 expression is involved in proliferation and invasion of lung squamous cell carcinoma. Oncotarget 7, 58470–58482. https://doi.org/10.18632/oncotarget.11298.

Sridhar, S., Schembri, F., Zeskind, J., Shah, V., Gustafson, A.M., Steiling, K., Liu, G., Dumas, Y.M., Zhang, X., Brody, J.S., Lenburg, M.E., Spira, A., 2008. Smoking-induced gene expression changes in the bronchial airway are reflected in nasal and buccal epithelium. BMC Genom. 9 https://doi.org/10.1186/1471-2164-9-259.

Sun, Y., Sheshadri, N., Zong, W.X., 2017. SERPINB3 and B4: From biochemistry to biology. Semin Cell Dev. Biol. 62, 170–177. https://doi.org/10.1016/j.semcdb.2016.09.005.

Trindade, F., Nogueira-Ferreira, R., Bastos, P., Amado, F., Ferreira, R., Vitorino, R., 2019. Bioinformatics to Tackle the Biological Meaning of Human Cerebrospinal Fluid Proteome. Methods Mol Biol. 2044, 393–553. https://doi.org/doi: 10.1007/978-1-4939-9706-0_26.

Turato, C., Pontisso, P., 2015. SERPINB3 (serpin peptidase inhibitor, clade B (ovalbumin) 3), Member. Atlas Genet Cytogenet Oncol. Haematol. 19, 202–209. https://doi.org/10.4267/2042/56413.

Uhlen, M., Zhang, C., Lee, S., Sjöstedt, E., Fagerberg, L., Bidkhori, G., Benfeitas, R., Arif, M., Liu, Z., Edfors, F., Sanli, K., Von Feilitzen, K., Oksvold, P., Lundberg, E., Hober, S., Nilsson, P., Mattsson, J., Schwenk, J.M., Brunnström, H., Glimelius, B., Sjöblom, T., Edqvist, P.H., Djureinovic, D., Micke, P., Lindskog, C., Mardinoglu, A., Ponten, F., 2017. A pathology atlas of the human cancer transcriptome. Science 357 (1979). https://doi.org/10.1126/science.aan2507.

Ullman, E., Pan, J.-A., Zong, W.-X., 2011. Squamous Cell Carcinoma Antigen 1 Promotes Caspase-8-Mediated Apoptosis in Response to Endoplasmic Reticulum Stress While Inhibiting Necrosis Induced by Lysosomal Injury. Mol. Cell Biol. 31, 2902–2919. https://doi.org/10.1128/mcb.05452-11.

Vital, N., Antunes, S., Louro, H., Vaz, F., Simões, T., Penque, D., Silva, M.J., 2021. Environmental Tobacco Smoke in Occupational Settings: Effect and Susceptibility Biomarkers in Workers From Lisbon Restaurants and Bars. Front Public Health 9. https://doi.org/10.3389/fpubh.2021.674142.

World Health Organization, 2019. WHO launches new report on global tobacco use trends [WWW Document]. News. URL https://www.who.int/news-room/detail/19-12-2019-who-launches-new-report-on-global-tobacco-use-trends (accessed 3.30.24).

Xu, Z., Wang, F., Gao, M., Chen, X., Hu, W., Xu, R., 2010. Targeting the Na(+)/K(+)-ATPase alpha1 subunit of hepatoma HepG2 cell line to induce apoptosis and cell cycle arresting. Biol. Pharm. Bull. 33, 743–751. https://doi.org/10.1248/bpb.33.743.

Yang, Z., Gao, S., Wong, C.C., Liu, W., Chen, H., Shang, H., Wu, Z.Y., Xu, L., Zhang, X., Wong, N., Kuang, M., Yu, J., 2023. TUBB4B is a novel therapeutic target in non-alcoholic fatty liver disease-associated hepatocellular carcinoma. J. Pathol. 260, 71–83. https://doi.org/10.1002/path.6065.

Zhuang, L., Xu, L., Wang, P., Jiang, Y., Yong, P., Zhang, C., Zhang, H., Meng, Z., Yang, P., 2015. Na + /K +-ATPase α1 subunit, a novel therapeutic target for hepatocellular carcinoma. Oncotarget 6, 28183–28193. https://doi.org/10.18632/oncotarget.4726.